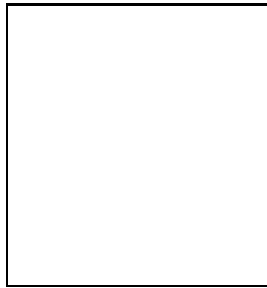


Evidence for Single Top Production at the Tevatron

Supriya Jain

*Homer L. Dodge Department of Physics and Astronomy, University of Oklahoma,
440 W. Brooks St., Norman, Oklahoma 73019, USA*

(On behalf of D0 and CDF Collaborations)



We present first evidence for the production of single top quarks at the Fermilab Tevatron $p\bar{p}$ collider. Both D0 and CDF experiments have measured the single top production cross section with a 3-standard-deviation significance using 0.9 fb^{-1} and 2.2 fb^{-1} of lepton+jets data, respectively. A direct measurement of the CKM matrix element that describes the Wtb coupling is also performed for the first time.

1 Introduction

The top quark was discovered in 1995 at the Tevatron¹ in pair production mode ($t\bar{t}$ events) involving strong interactions. But the standard model (SM) also predicts the production of single top quarks through the electroweak exchange of a W boson. At the Tevatron, the s - and t -channel production modes illustrated in Fig. 1 are dominant. An observation of single top production is interesting since it would provide a direct measurement of the CKM matrix element $|V_{tb}|$ and top quark polarization, in addition to probing possible new physics in the top quark sector. But observing single top quarks is challenging on account of smaller cross sections (about half that of $t\bar{t}$ production) as well as larger backgrounds on account of only one massive object in the final state. The total predicted cross section for single top quarks at the Tevatron is $2.86 \pm 0.33 \text{ pb}^2$ for a top quark mass of 175 GeV. Simple selections that exploit kinematic features of the signal final state are not sufficient, and one needs sophisticated multivariate techniques to separate single top events from the overwhelming backgrounds. Both D0 and CDF have performed several multivariate analyses^{3,4} to identify the putative signal in data, and we report here the results.

2 Event Selections

The experimental signal for single top quark events consists of one isolated high transverse momentum, central pseudorapidity charged lepton (electron e or muon μ) and missing transverse

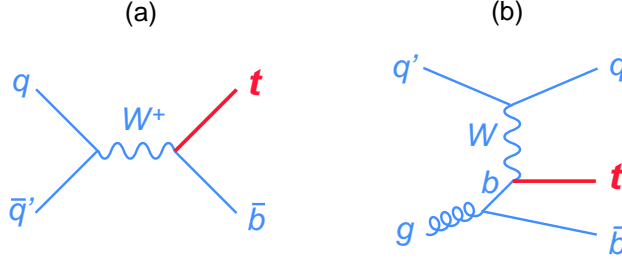


Figure 1: Representative Feynman diagrams for (a) s-channel and (b) t-channel single top quark production.

energy from the decay of a W boson from the top quark decay, accompanied by a b jet also from the top quark decay. There is always a second jet, which originates from a b quark produced with the top quark in the s-channel, or which comes from a forward-traveling up- or down-type quark in t-channel events. Some t-channel events have a detectable b jet from the gluon splitting to $b\bar{b}$. Both D0 and CDF apply selections to keep signal-like events while rejecting backgrounds. CDF includes events with two or three jets with single or double b -tags, while D0 includes four-jet events also in which the additional jet is from initial-state or final-state radiation.

3 Signal and Background Modeling

Modeling of signals and backgrounds is done using both Monte Carlo simulations and data. The main backgrounds are: W +jets; $t\bar{t}$ in the lepton+jets and dilepton final states, when a jet or a lepton is not reconstructed; and multijet production, where a jet is misreconstructed as an electron or a heavy-flavor quark decays to a muon that is misidentified as isolated from the jet. The W +jets includes both W +light-flavor jets (Wjj) and W +heavy-flavor jets ($Wb\bar{b}$, $Wc\bar{c}$, and Wcj). There is also a small contribution from diboson and Z +jets events. D0 analysed 0.9 fb^{-1} of lepton+jets data, while CDF analyzed 2.2 fb^{-1} of data. The expected and observed event yields from both experiments after all selections are shown in Table 1.

Table 1: Event yields, (left) at D0, 0.9 fb^{-1} , and (right) at CDF, 2.2 fb^{-1} , for e and μ , 1 b tag and 2 b tag channels summed. The diboson and Z +jets events are included in the overall W +jets background at D0.

Source	2 jets	3 jets	4 jets	Source	2 jets	3 jets
tb	16 ± 3	8 ± 2	2 ± 1	tb	41.2 ± 5.9	13.5 ± 1.9
tqb	20 ± 4	12 ± 3	4 ± 1	tqb	62.1 ± 9.1	18.3 ± 2.7
$t\bar{t}$	59 ± 10	135 ± 26	154 ± 33	$t\bar{t}$	146.0 ± 20.9	338.7 ± 48.2
$Wb\bar{b}$	261 ± 55	120 ± 24	35 ± 7	$Wb\bar{b}$	461.6 ± 139.7	141.1 ± 42.6
$Wc\bar{c}, Wcj$	151 ± 31	85 ± 17	23 ± 5	$Wc\bar{c}, Wcj$	395.0 ± 121.8	108.8 ± 33.5
Wjj	119 ± 25	43 ± 9	12 ± 2	Wjj	339.8 ± 56.1	101.8 ± 16.9
Multijets	95 ± 19	77 ± 15	29 ± 6	Multijets	59.5 ± 23.8	21.3 ± 8.5
Total background	686 ± 41	460 ± 39	253 ± 38	Diboson	63.2 ± 6.3	21.5 ± 2.2
Data	697	455	246	Z +jets	26.7 ± 3.9	11.0 ± 1.6
				Total background	1491.8 ± 268.6	754.8 ± 91.3
				Data	1535	712

4 Cross Section Measurements at D0

Three different multivariate analyses were performed at D0 in order to separate the single top signal from backgrounds: boosted decision trees (DT), Bayesian neural networks (BNN), and

matrix elements (ME). The discriminants from each analysis are shown in Fig. 2. Cross section measurements are extracted from a binned likelihood of the discriminants separately for each analysis. The results are then combined using the BLUE (best linear unbiased estimate) method yielding $\sigma(p\bar{p} \rightarrow tb + X, tqb + X) = 4.7 \pm 1.3 \text{ pb}$. A large ensemble of pseudo-datasets is created to estimate the significance of measurements. It is:

$$\begin{aligned} \text{Expected p-value} &: 1.1\% \quad (2.3 \text{ standard deviations}) \\ \text{Observed p-value} &: 0.014\% \quad (3.6 \text{ standard deviations}). \end{aligned}$$

Additionally, D0 also measured the value of $|V_{tb}|$ using two different assumptions for the prior probability density of $|V_{tb}|^2$ as shown in Fig 3.

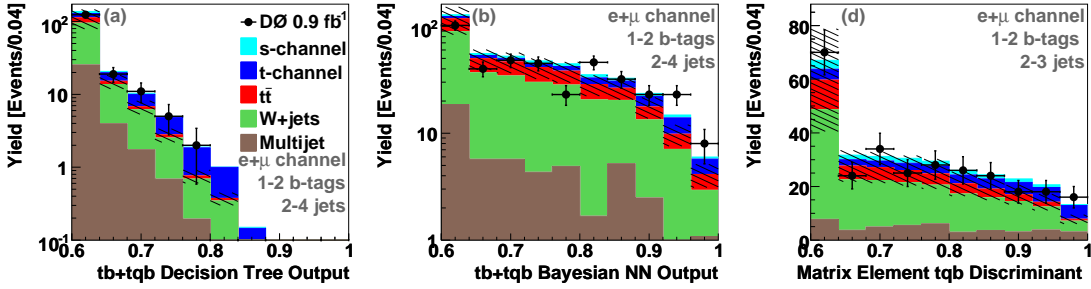


Figure 2: The signal regions of the multivariate discriminants at D0: (a) DT, (b) BNN, and (c) ME.

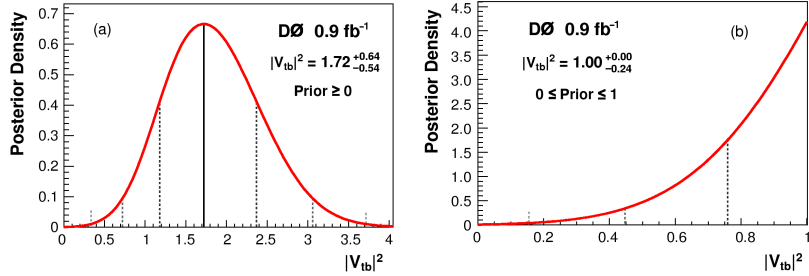


Figure 3: The Bayesian posterior density distributions for $|V_{tb}|^2$ for (a) $\text{prior} \geq 0$, and (b) $0 \leq \text{prior} \leq 1$ at D0. The dashed lines show the positions of the one, two, and three standard deviations away from the peak of each curve.

5 Cross Section Measurements at CDF

CDF performed the following multivariate analyses: likelihood function (LF), neural networks (NN), and matrix elements (ME). The discriminants from each analysis are shown in Fig. 4. Subsequent cross section measurements using a binned likelihood are the following:

$$\begin{aligned} \sigma(p\bar{p} \rightarrow \mathbf{tb} + \mathbf{X}, \mathbf{tqb} + \mathbf{X}) &= 1.8_{-0.8}^{+0.9} \text{ pb} \quad (\text{Likelihood function}) \\ &= 2.0_{-0.8}^{+0.9} \text{ pb} \quad (\text{Neural networks}) \\ &= 2.2_{-0.7}^{+0.8} \text{ pb} \quad (\text{Matrix elements}). \end{aligned}$$

From the above results, $|V_{tb}|$ is measured to be $0.78_{-0.21}^{+0.18}$, and a lower limit of 0.41 is also set at 95% confidence level (CL).

6 Single Top Projections

D0 and CDF also made projections for different measurements based on their current analyses. The allowed contours at 68% and 95% CL in a two-dimensional plane of σ_s versus σ_t , and the

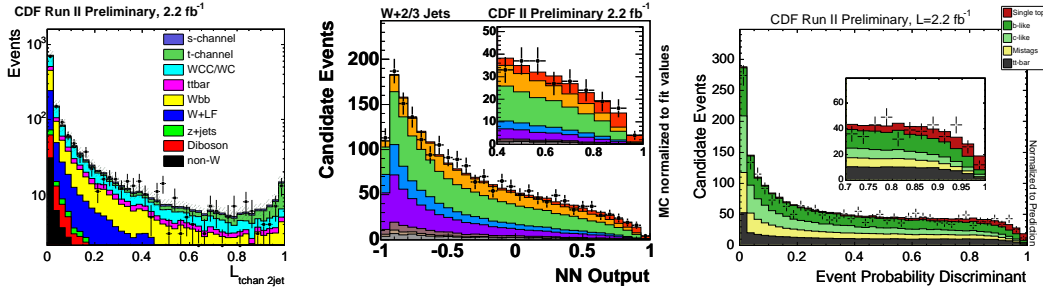


Figure 4: Multivariate discriminant output distributions at CDF: LF (left), NN (middle), and ME (right).

uncertainty on $|V_{tb}|$, expected at different values of integrated luminosity are shown in Fig. 5. We see that it is possible to exclude several models beyond SM at about 7 fb^{-1} , and $|V_{tb}|$ can be measured with a precision better than 10% as the Tevatron collects more data.

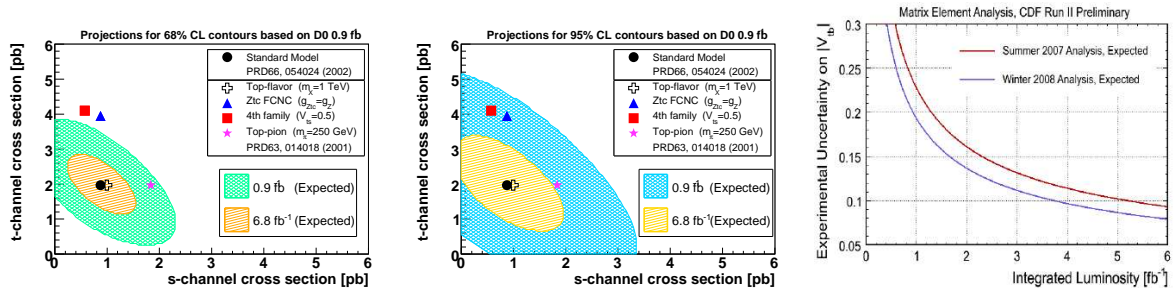


Figure 5: The allowed contours at 68% and 95% CL in a two-dimensional plane of σ_s versus σ_t , and the uncertainty on $|V_{tb}|$ expected at different values of integrated luminosity based on D0 and CDF data.

7 Summary

To conclude, searches for single top quarks have been performed at the Tevatron using multivariate techniques to separate the signal from the huge backgrounds. Both D0 and CDF have measured the single top production cross section with a 3-standard-deviation significance using 0.9 fb^{-1} and 2.2 fb^{-1} of lepton+jets data, respectively. A direct measurement of the CKM matrix element $|V_{tb}|$ is also performed for the first time. As the Tevatron collects more data, both experiments continue to improve their analyses in order to increase the sensitivity to a possible observation.

Acknowledgments

The author would like to thank the organizers for creating a fruitful collaborative environment at the conference, and also the European Union for their support under the Marie Curie programme.

References

1. F. Abe *et al.* (CDF Collaboration), Phys. Rev. Lett. **74**, 2626 (1995); S. Abachi *et al.* (D0 Collaboration), *ibid.* **74**, 2632 (1995).
2. Z. Sullivan, Phys. Rev. D **70**, 114012 (2004).
3. CDF Conference Note 9221, Feb., 2008; CDF Conference Note 9217, Mar., 2008; CDF Conference Note 9223, Feb., 2008.
4. V.M. Abazov *et al.* [DØCollaboration], Phys. Rev. Lett. **98**, 181902 (2007); V.M. Abazov *et al.* (D0 Collaboration), accepted by Phys. Rev. D, arXiv:0803.0739.